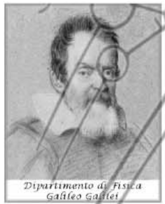

Ion-channelling at MeV energies: a tool for a detailed investigation of crystal structures

Alberto Carnera
Dipartimento di Fisica - Univ. Padova
&
INFN-Laboratori Nazionali di Legnaro

W.Brandt, Scientific American 218, 90 , 1968

Introduction

Introduction

Schematics of the experiment

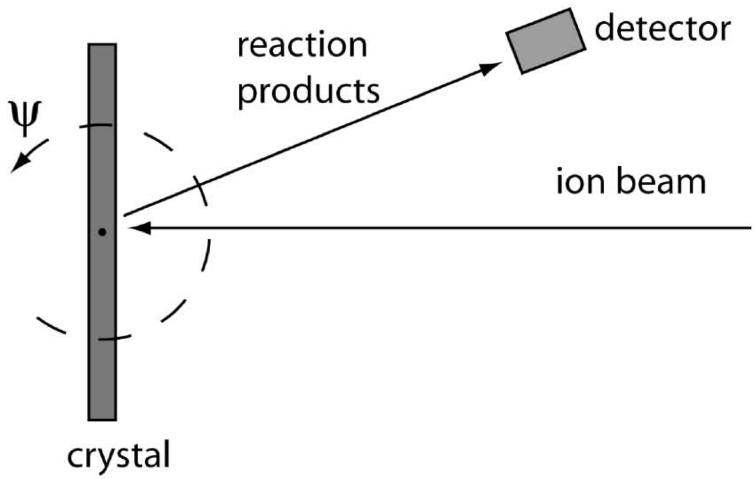

Introduction

Schematics of the experiment

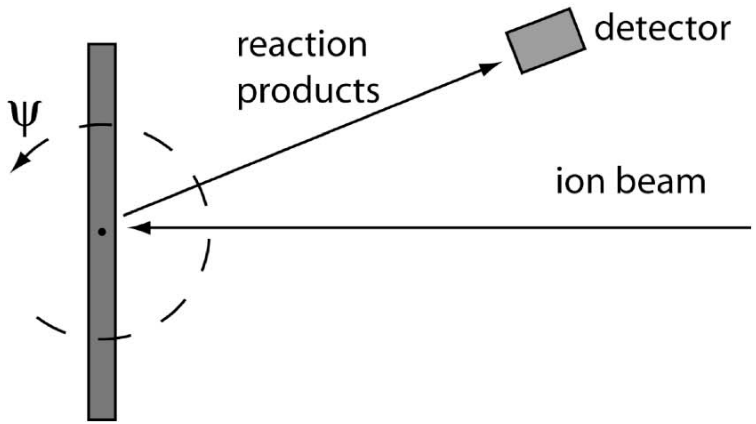

The yield of the reaction products detected can be written as:

$$Y(\psi) \propto P_{ce}(\psi) = \int P_M(\mathbf{r}) F(\psi, \mathbf{r}) d\mathbf{r}$$

Introduction

Schematics of the experiment

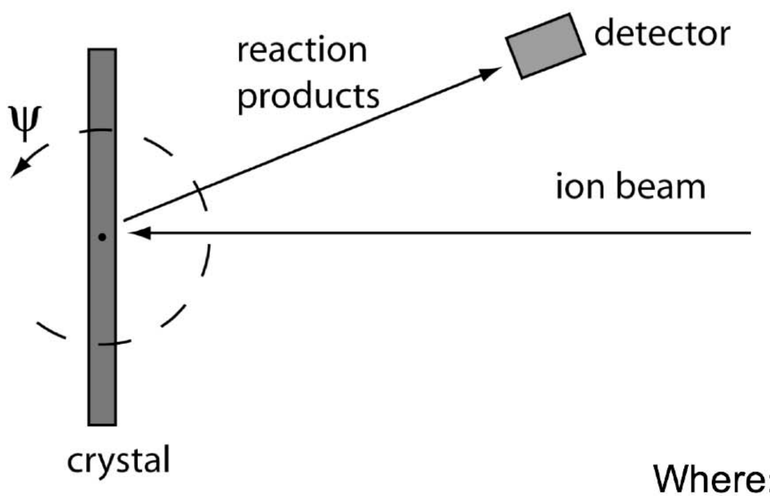

The yield of the reaction products detected can be written as:

$$Y(\psi) \propto P_{ce}(\psi) = \int P_M(\mathbf{r}) F(\psi, \mathbf{r}) d\mathbf{r}$$

Where:

$Y(\psi)$: Yield of the reaction products as the function of the rotation angle

Introduction

Schematics of the experiment

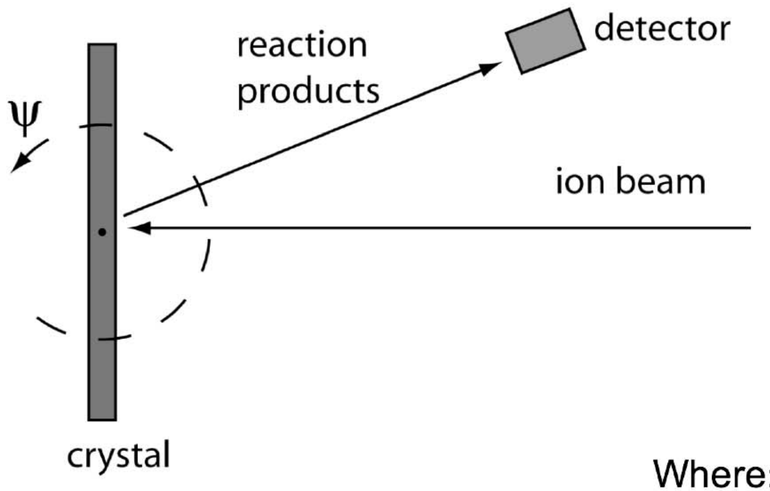

The yield of the reaction products detected can be written as:

$$Y(\psi) \propto P_{ce}(\psi) = \int P_M(\mathbf{r}) F(\psi, \mathbf{r}) d\mathbf{r}$$

Where:

$Y(\psi)$: Yield of the reaction products as the function of the rotation angle

$P_{ce}(\psi)$: close encounter probability

Introduction

Schematics of the experiment

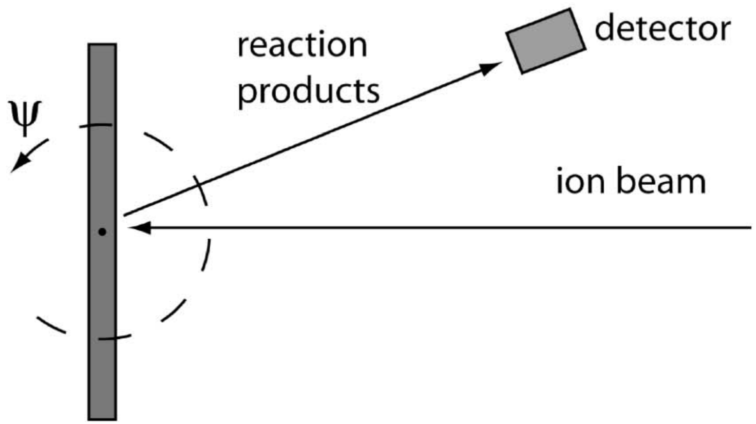

The yield of the reaction products detected can be written as:

$$Y(\psi) \propto P_{ce}(\psi) = \int P_M(\mathbf{r}) F(\psi, \mathbf{r}) d\mathbf{r}$$

Where:

$Y(\psi)$: Yield of the reaction products as the function of the rotation angle

$P_{ce}(\psi)$: close encounter probability

$F(\psi, \mathbf{r})$: ion flux at position $\mathbf{r}$ within the crystal

Introduction

Schematics of the experiment

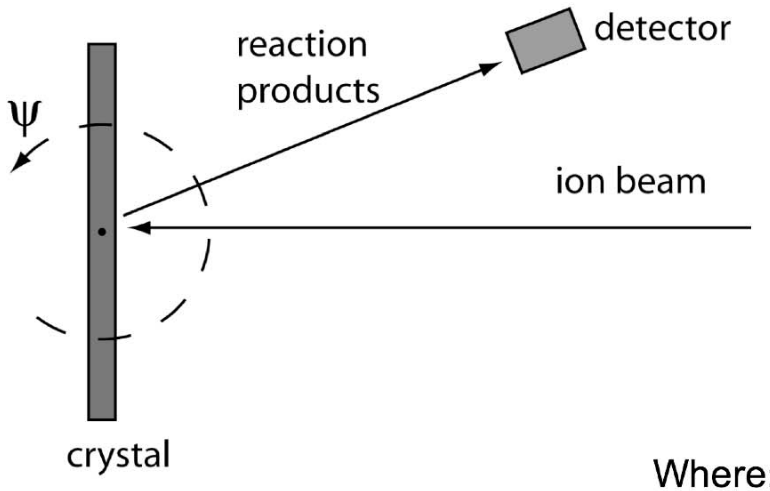

The yield of the reaction products detected can be written as:

$$Y(\psi) \propto P_{ce}(\psi) = \int P_M(\mathbf{r}) F(\psi,\mathbf{r}) d\mathbf{r}$$

Where:

$Y(\psi)$: Yield of the reaction products as the function of the rotation angle

$P_{ce}(\psi)$: close encounter probability

$F(\psi,\mathbf{r})$: ion flux at position $\mathbf{r}$ within the crystal

$P_M(\mathbf{r})$: probability for a specific nucleus to be at $\mathbf{r}$ (crystal lattice description)

Introduction

Schematics of the experiment

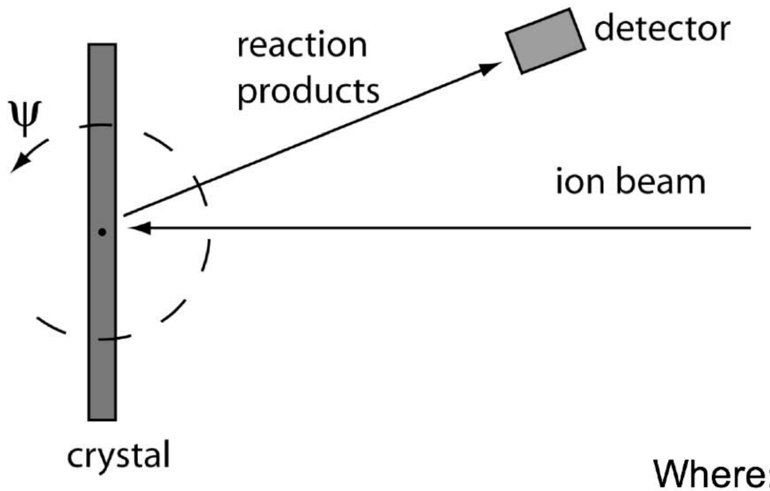

The yield of the reaction products detected can be written as:

$$Y(\psi) \propto P_{ce}(\psi) = \int P_M(\mathbf{r}) F(\psi, \mathbf{r}) d\mathbf{r}$$

Where:

$Y(\psi)$: Yield of the reaction products as the function of the rotation angle

$P_{ce}(\psi)$: close encounter probability

$F(\psi, \mathbf{r})$: ion flux at position $\mathbf{r}$ within the crystal

$P_M(\mathbf{r})$: probability for a specific nucleus to be at $\mathbf{r}$ (crystal lattice description)

Basic features

Basic features

- The interaction is intrinsically local (nuclear or atomic)

Basic features

- The interaction is intrinsically local (nuclear or atomic)
  - elastic Rutherford scattering (RBS)

Basic features

- The interaction is intrinsically local (nuclear or atomic)
  - elastic Rutherford scattering (RBS)
  - nuclear reactions (NRA)

Basic features

- The interaction is intrinsically local (nuclear or atomic)
  - elastic Rutherford scattering (RBS)
  - nuclear reactions (NRA)
  - electronic excitations (PIXE)

Basic features

- The interaction is intrinsically local (nuclear or atomic)
  - elastic Rutherford scattering (RBS)
  - nuclear reactions (NRA)
  - electronic excitations (PIXE)
- The detected signal is Z (& sometimes M) selective

Basic features

- The interaction is intrinsically local (nuclear or atomic)
  - elastic Rutherford scattering (RBS)
  - nuclear reactions (NRA)
  - electronic excitations (PIXE)
- The detected signal is Z (& sometimes M) selective
  - a single sublattice can be selectively studied

Basic features

- The interaction is intrinsically local (nuclear or atomic)
  - elastic Rutherford scattering (RBS)
  - nuclear reactions (NRA)
  - electronic excitations (PIXE)
- The detected signal is Z (& sometimes M) selective
  - a single sublattice can be selectively studied
- The signal can be often resolved in depth

Basic features

- The interaction is intrinsically local (nuclear or atomic)
  - elastic Rutherford scattering (RBS)
  - nuclear reactions (NRA)
  - electronic excitations (PIXE)
- The detected signal is Z (& sometimes M) selective
  - a single sublattice can be selectively studied
- The signal can be often resolved in depth
  - different layers can be distinguished

Basic features

- The interaction is intrinsically local (nuclear or atomic)
  - elastic Rutherford scattering (RBS)
  - nuclear reactions (NRA)
  - electronic excitations (PIXE)
- The detected signal is Z (& sometimes M) selective
  - a single sublattice can be selectively studied
- The signal can be often resolved in depth
  - different layers can be distinguished
- The De Broglie wavelength is much smaller than the lattice constants

Basic features

- The interaction is intrinsically local (nuclear or atomic)
  - elastic Rutherford scattering (RBS)
  - nuclear reactions (NRA)
  - electronic excitations (PIXE)
- The detected signal is Z (& sometimes M) selective
  - a single sublattice can be selectively studied
- The signal can be often resolved in depth
  - different layers can be distinguished
- The De Broglie wavelength is much smaller than the lattice constants
  - diffraction effects can be disregarded: lattice description in the direct space

Basic features

- The interaction is intrinsically local (nuclear or atomic)
  - elastic Rutherford scattering (RBS)
  - nuclear reactions (NRA)
  - electronic excitations (PIXE)
- The detected signal is Z (& sometimes M) selective
  - a single sublattice can be selectively studied
- The signal can be often resolved in depth
  - different layers can be distinguished
- The De Broglie wavelength is much smaller than the lattice constants
  - diffraction effects can be disregarded: lattice description in the direct space
  - even isolated atoms can be located in the lattice

Experimental apparatus
&
Methods

RBS-NRA-PIXE channeling apparatus

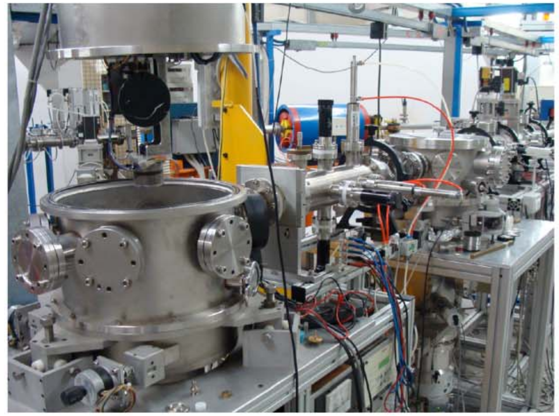

Chamber for channeling experiments at AN-2000 - Laboratori Nazionali di Legnaro

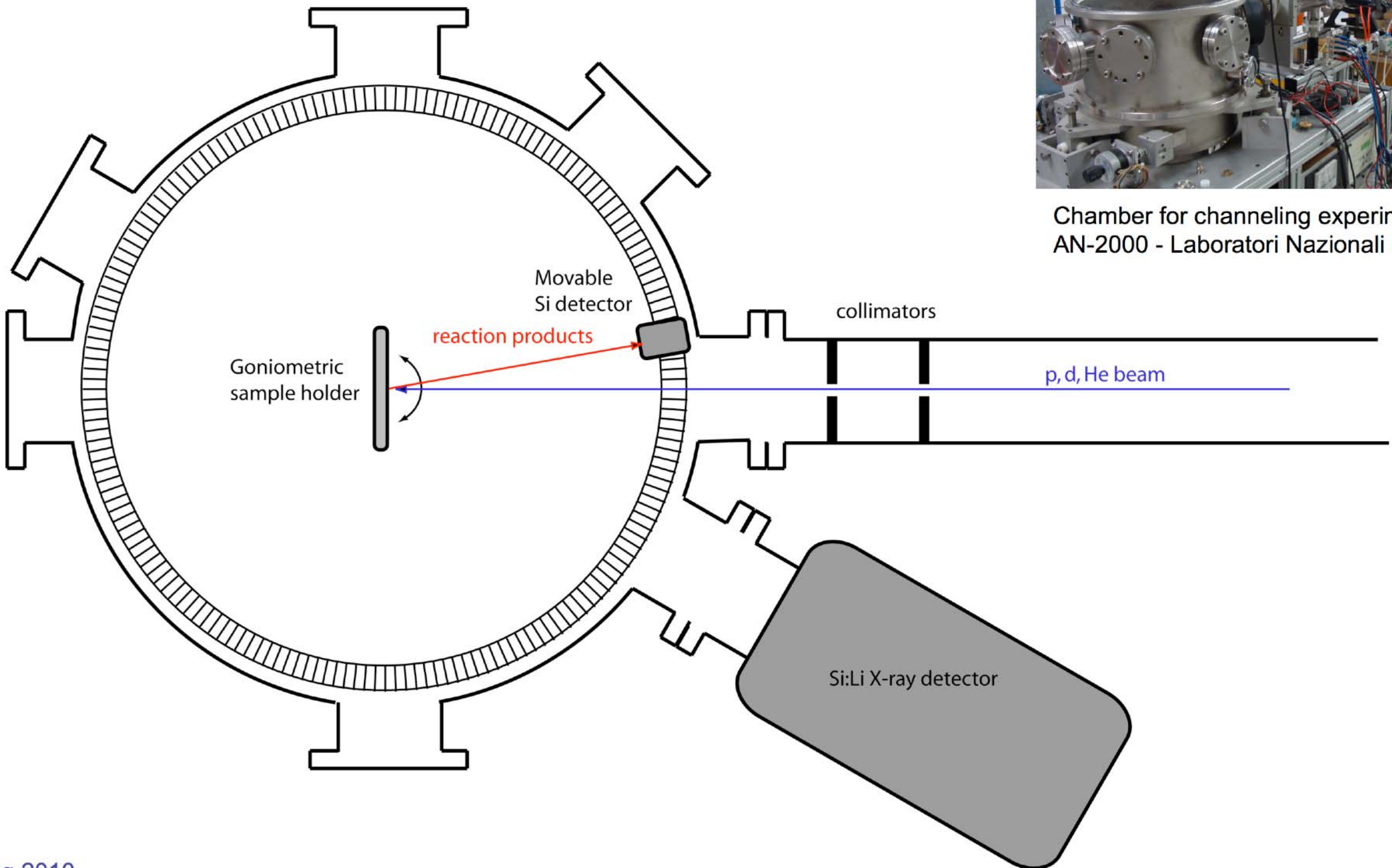

The goniometer for RBS & NRA channeling studies

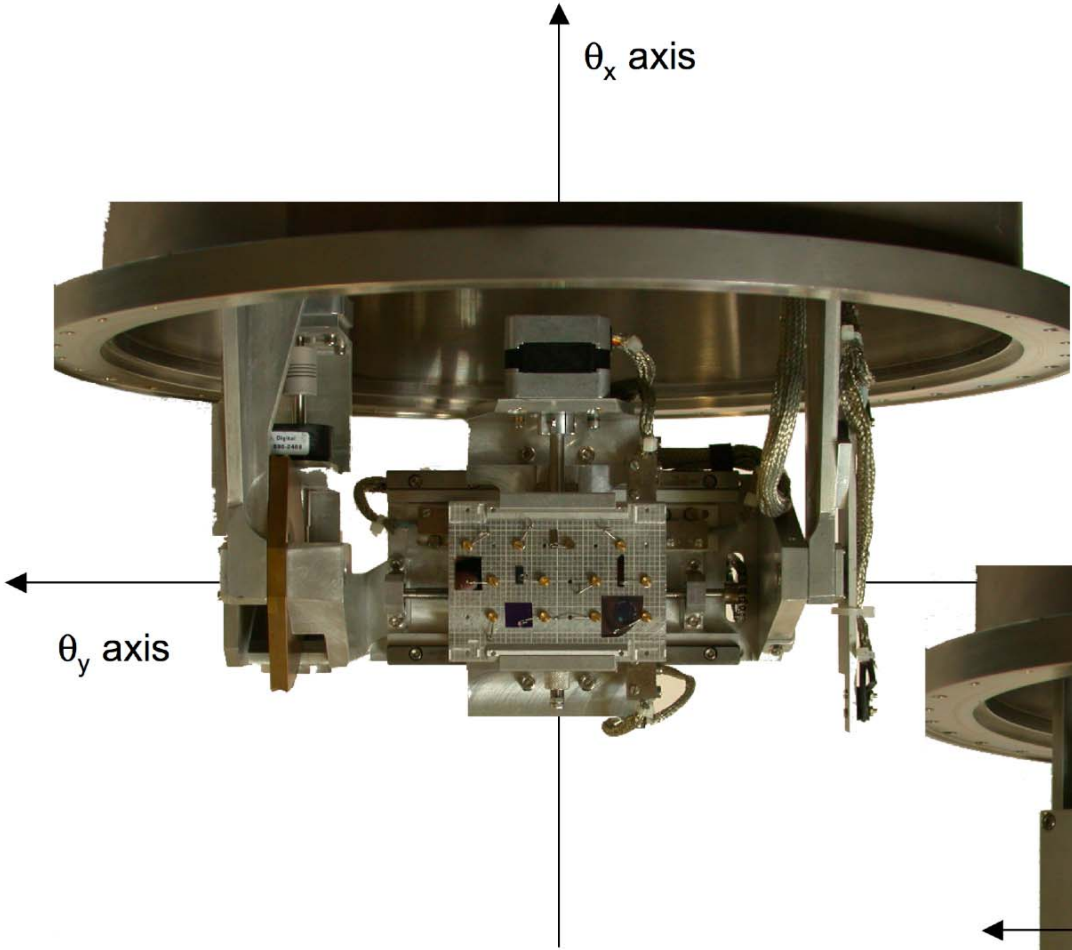

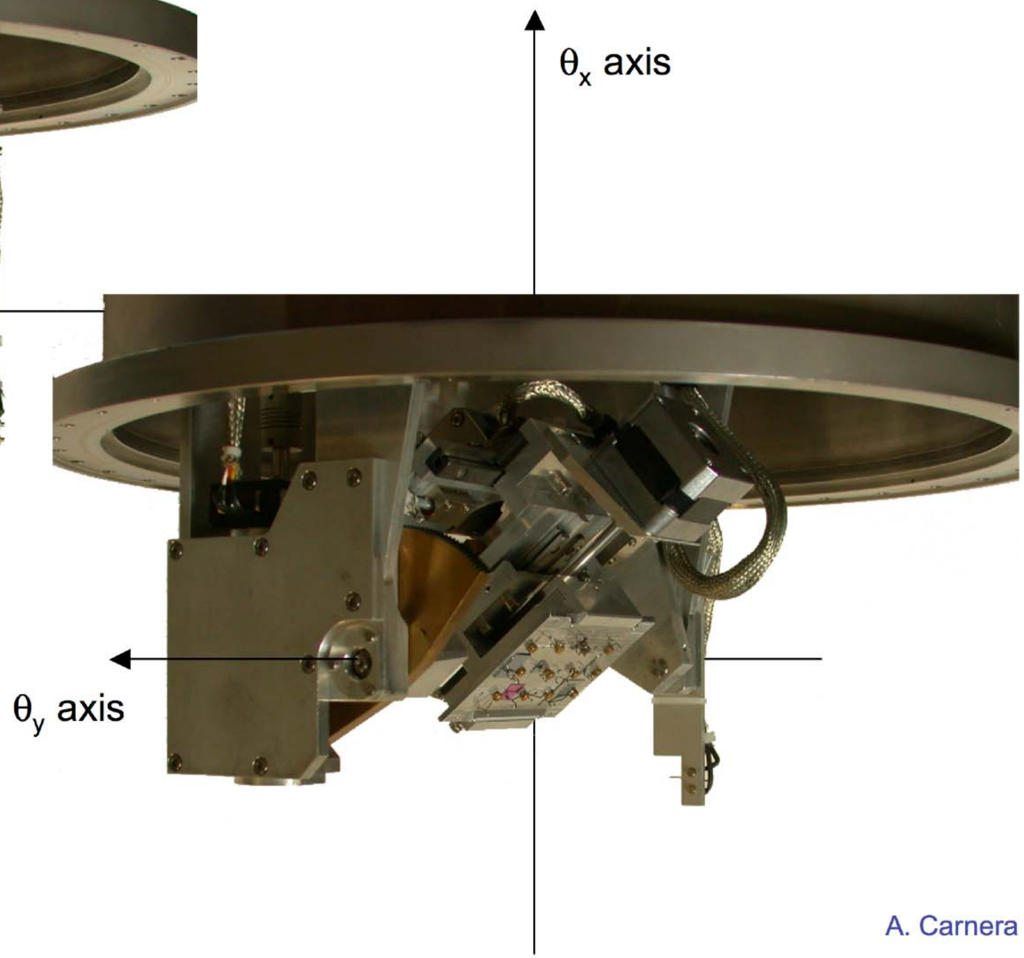

Ang. resolution 0.01° (≈0.2 mrad)
Minimum pressure ≈10^{-7} mbar

RBS-channeling spectra

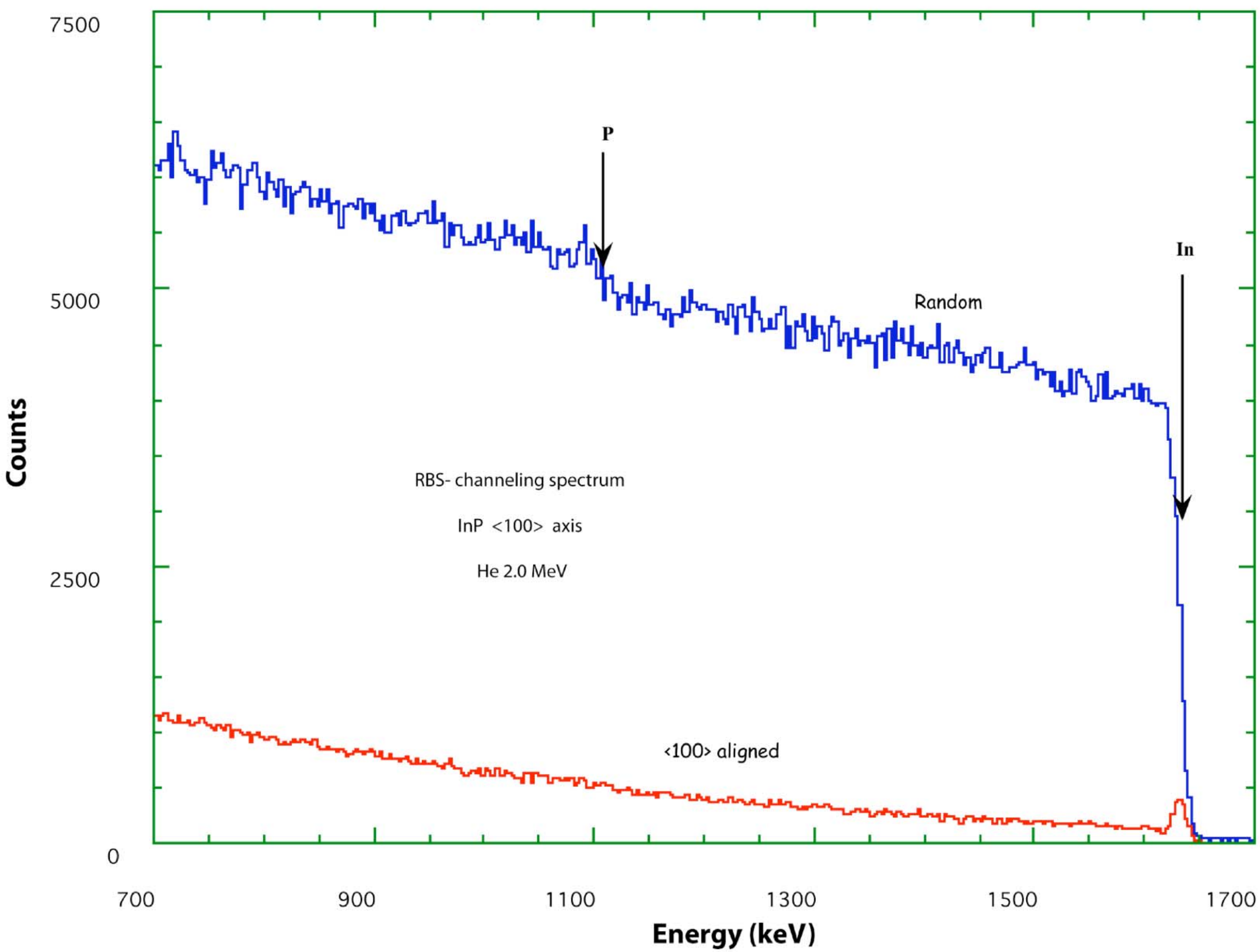

Crystal planes mapping around an axis

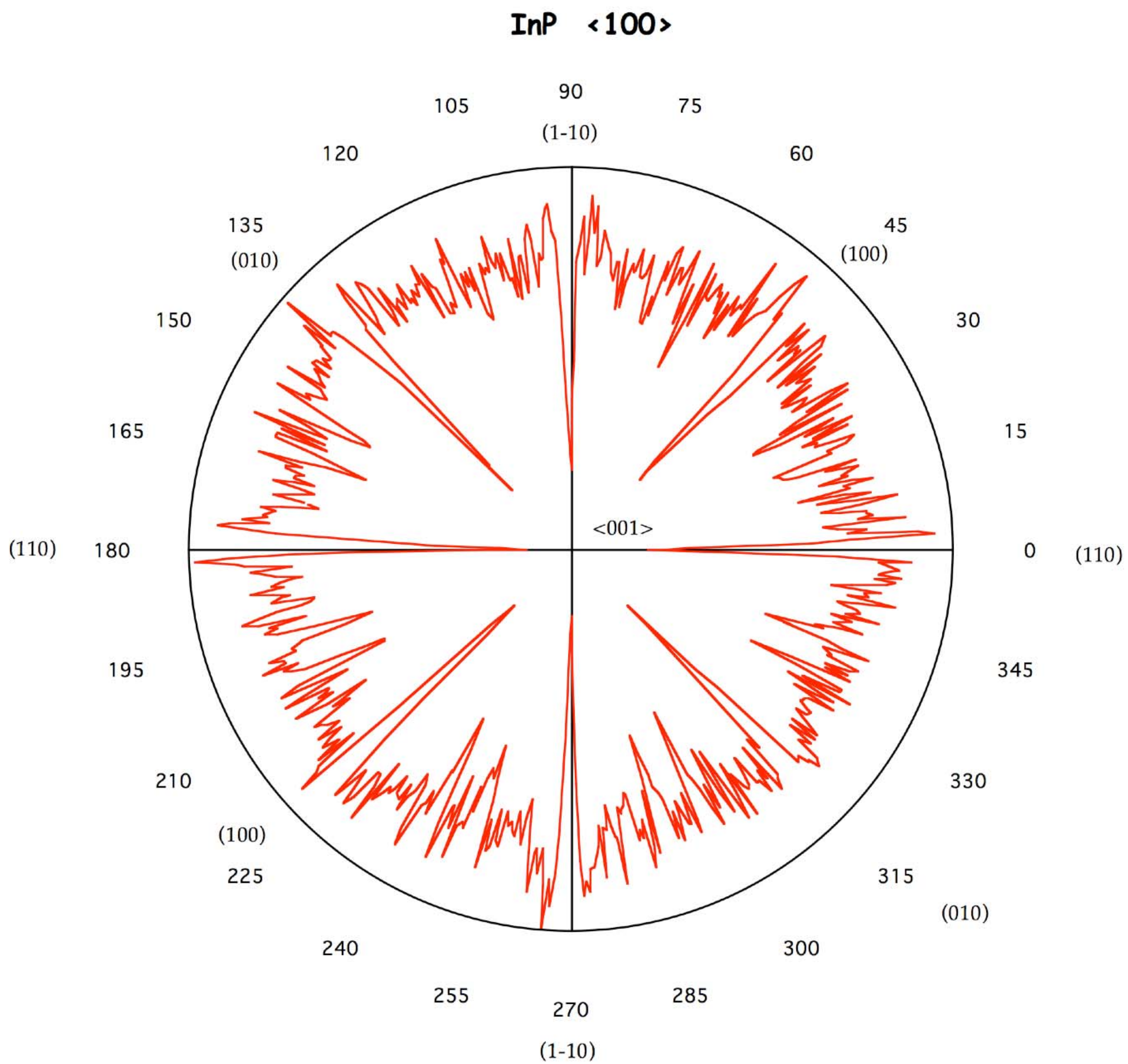

Axes mapping within a (110) plane

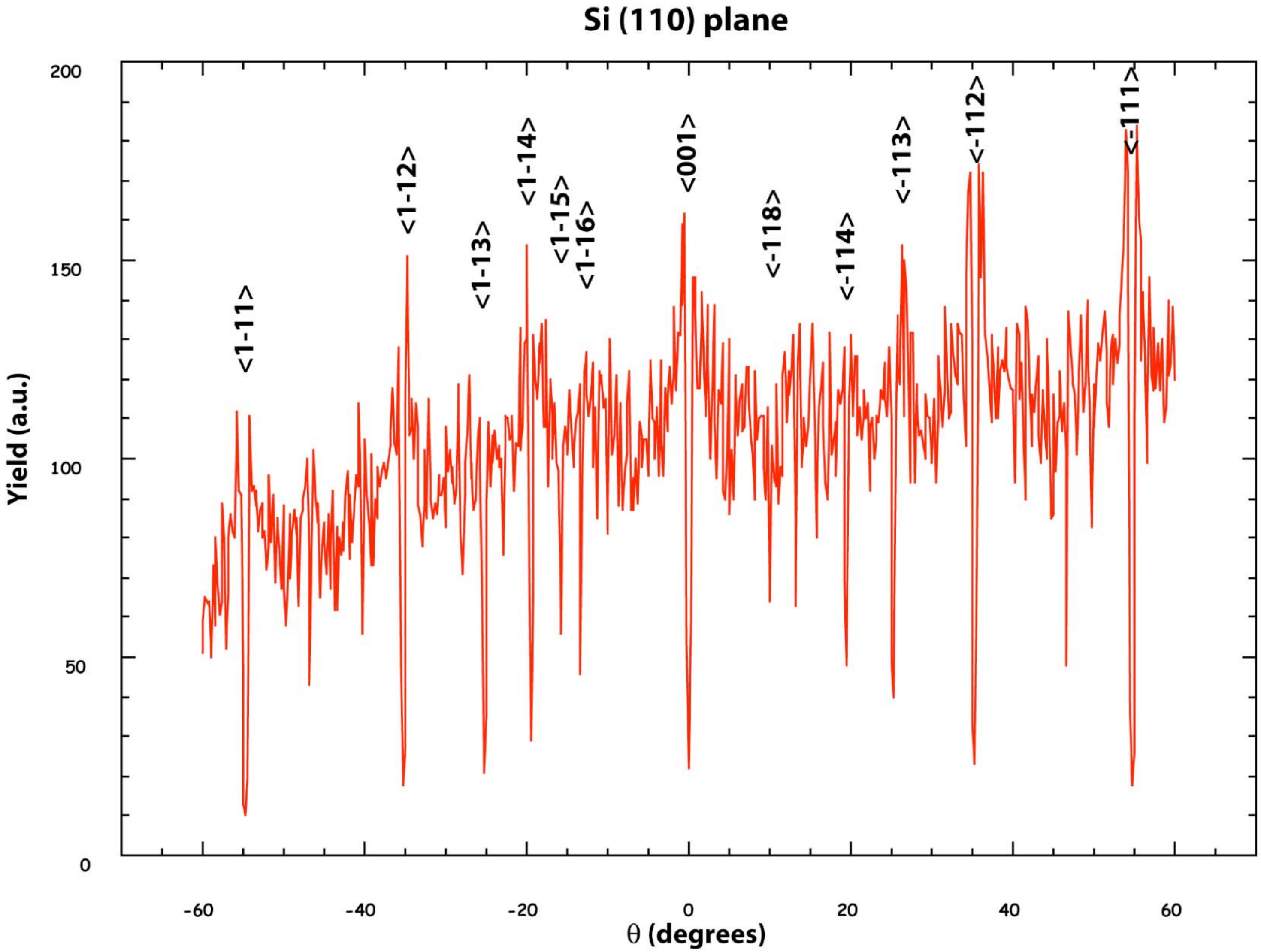

Crystalline defects studies

Amorphous layers studies

<001> aligned spectra for 2 MeV ^{4}He ions on Si implanted at LN temperature and then annealed for increasing times at 550 °C.

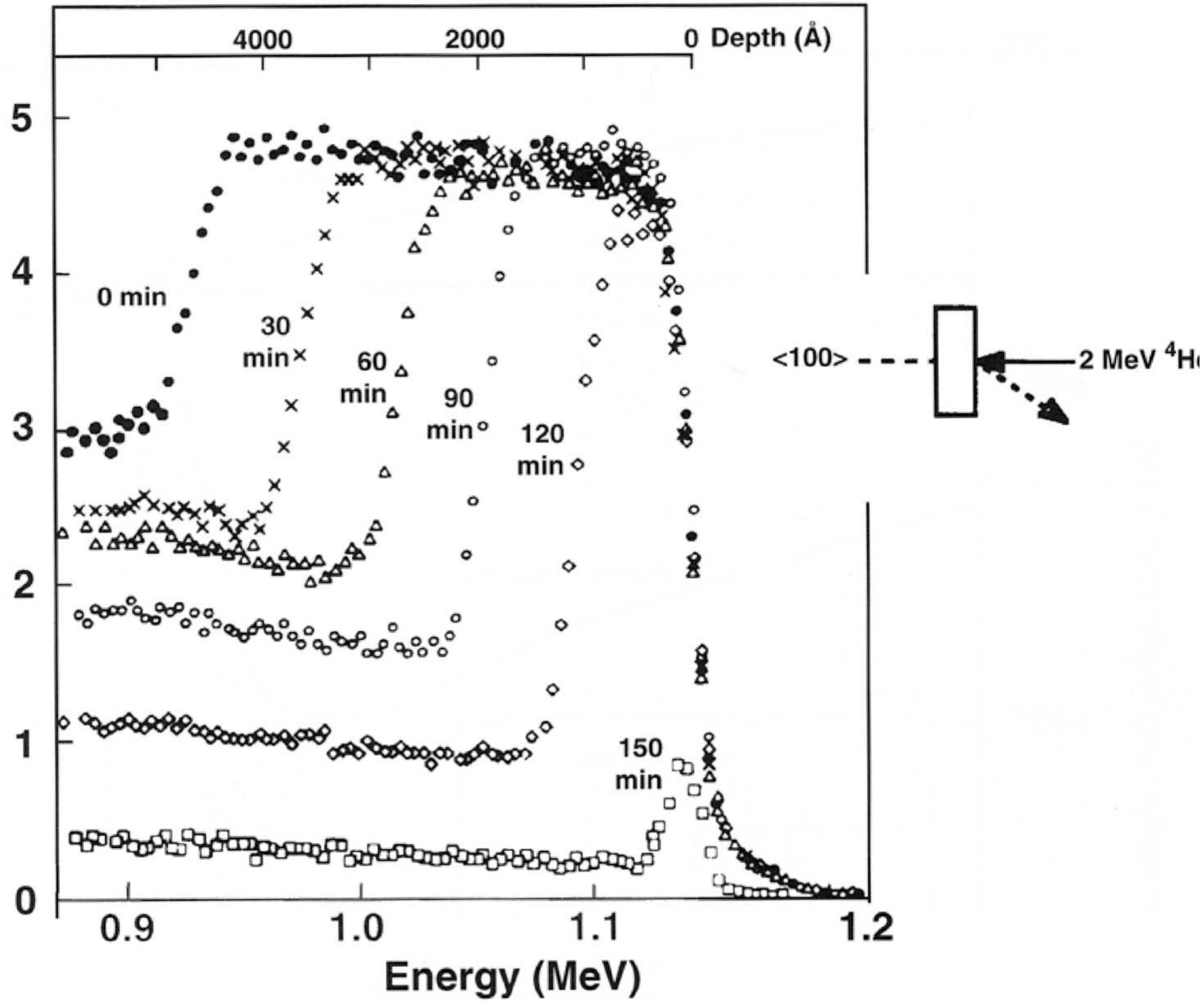

Csepregi, Mayer, Sigmon Appl.Phys.Lett. 29, 92, 1976

Substitutional impurities (dopants)

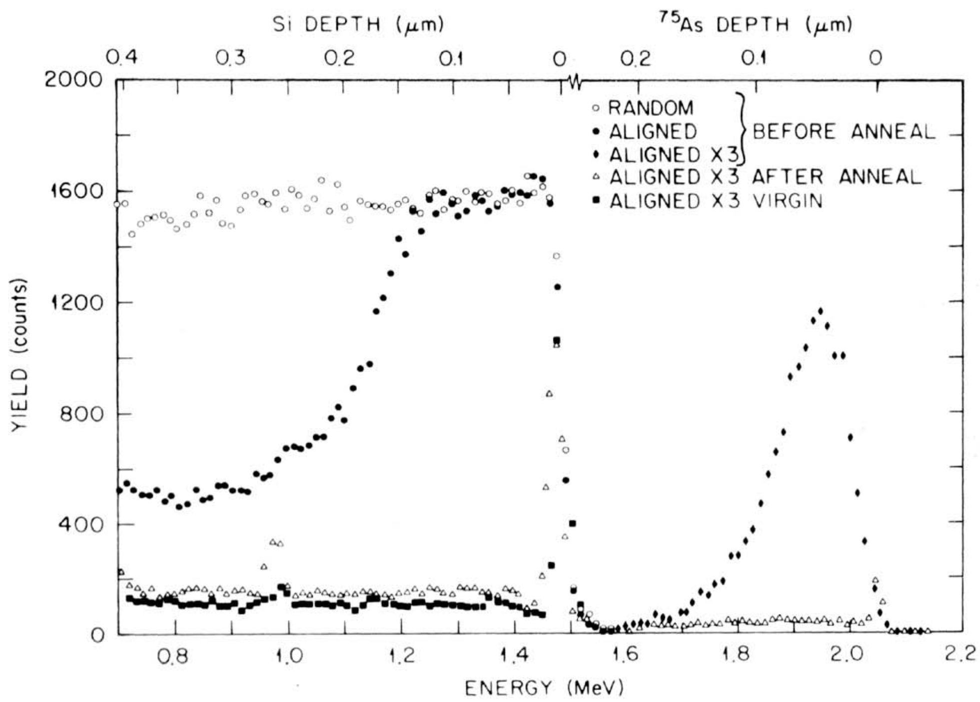

150 keV, 1.4x10^{16} As/cm^2

White, Pronko, Wilson, Appleton, Narayan and Young J.Appl.Phys. 50, 3261 (1979)

Substitutional impurities (dopants)

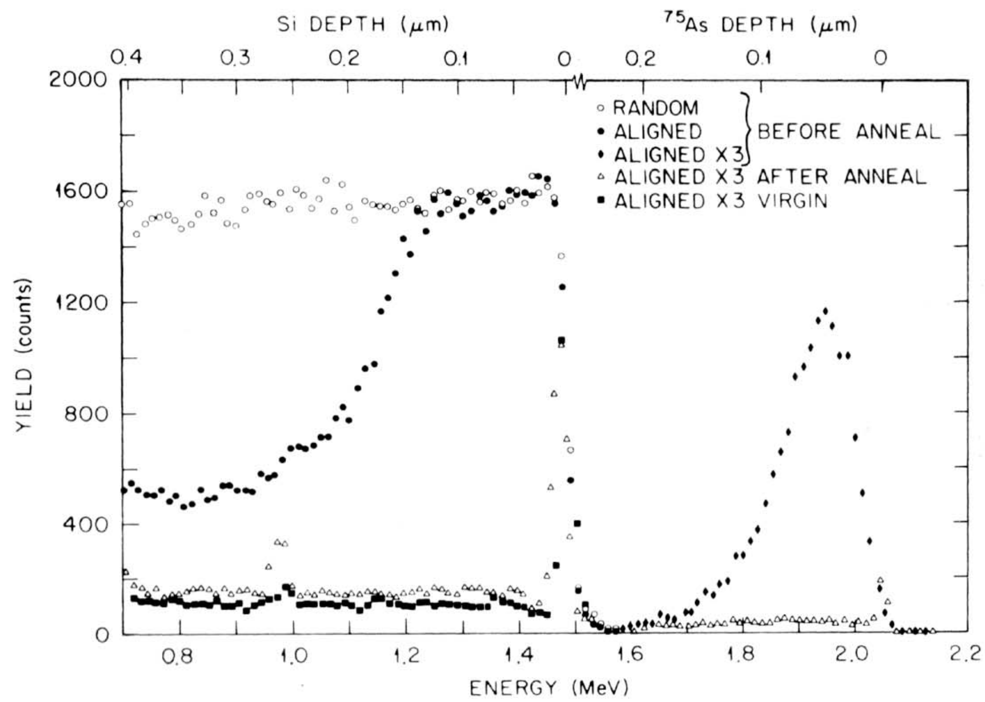

150 keV, 1.4x10^{16} As/cm^2

White, Pronko, Wilson, Appleton, Narayan and Young J.Appl.Phys. 50, 3261 (1979)

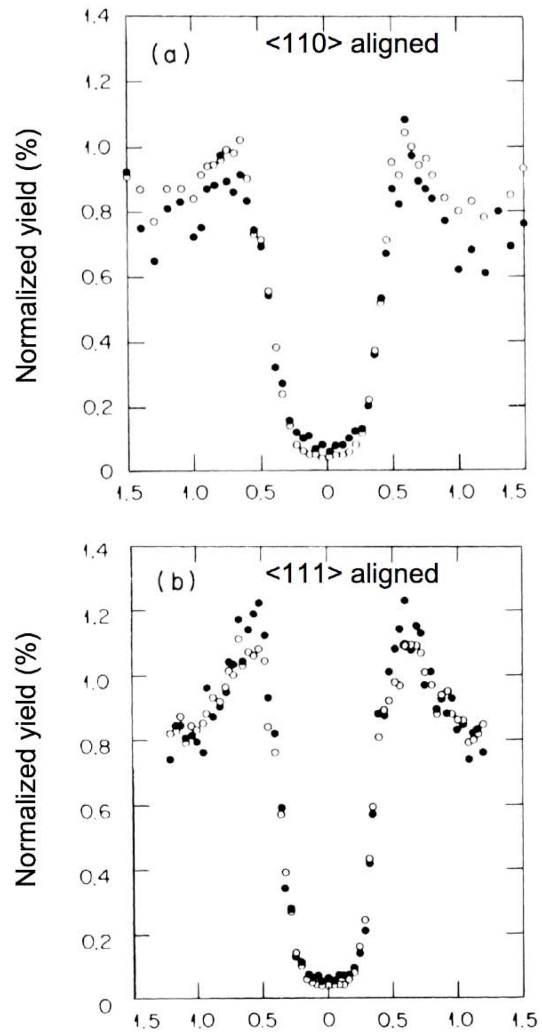

Tilt angle (degrees)

Epiataxial layers

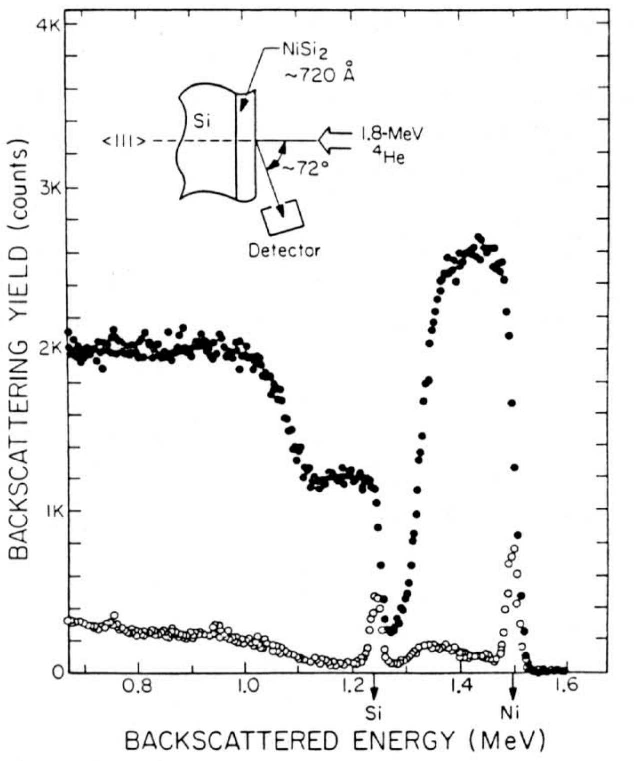

Random and <111> spectra from a $NiSi_2$ epitaxial layer on a Si (111) substrate

Chu, Poate, Feldman and Doherty Appl.Phys.Lett 36, 544, 1980

Epiataxial layers

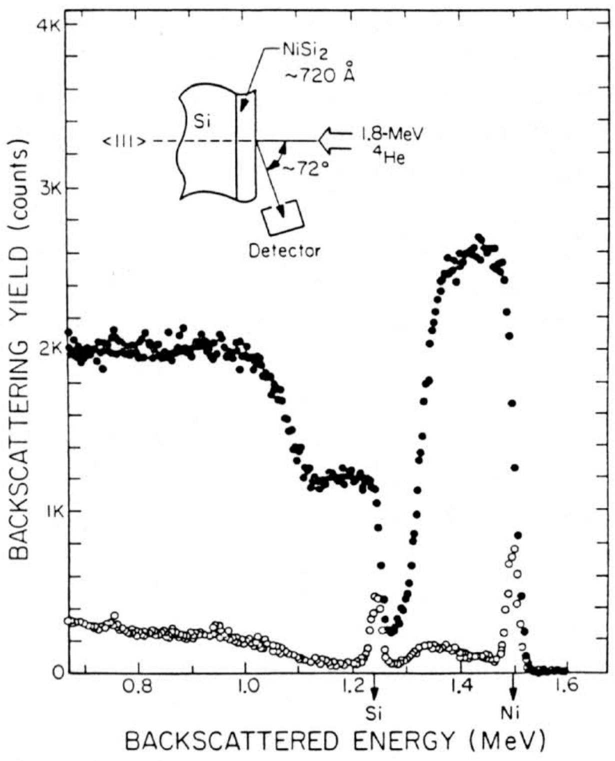

Random and <111> spectra from a $NiSi_2$ epitaxial layer on a Si (111) substrate

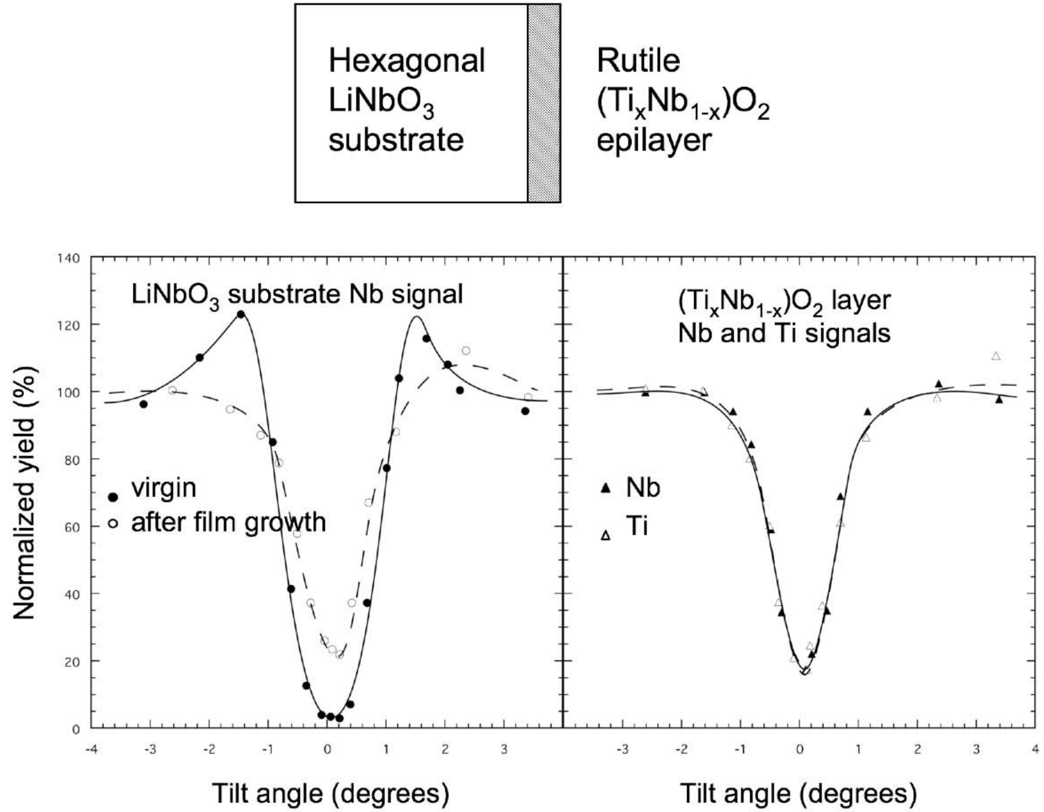

Channeling dips showing the perfect epitaxial growth of the $(Ti_xNb_{1-x})O_2$ phase on an $LiNbO_3$ substrate

Chu, Poate, Feldman and Doherty Appl.Phys.Lett 36, 544, 1980

Armenise, Canali, De Sario, Carnera, Mazzoldi and Celotti JAP 54, 62, 1983

Dechanneling by dislocations

Single layer $In_xGa_{1-x}As/GaAs$ strained structure TEM images

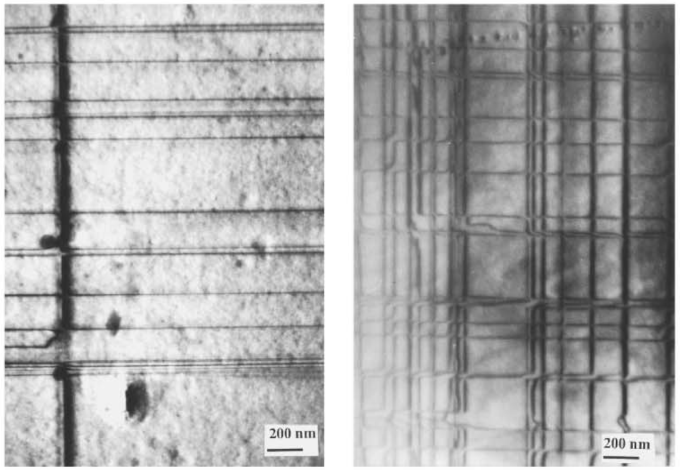

(a) (b)

(001) plan view bright-field zone axis TEM micrographs of two $In_xGa_{1-x}As/GaAs$ layers showing the different MD densities along the two <110>-type directions: (a) sample 2, x=0.105, t=68 nm; (b) sample 3, x=0.080, t=200 nm. It is worth noting that the dislocations tend to align in bands even at low density.

Mazzer, Drigo, Romanato, Salviati and Lazzarini PRB 56, 6895,1997

Dechanneling by dislocations

Single layer InxGa$_{1-x}$As/GaAs strained structure TEM images

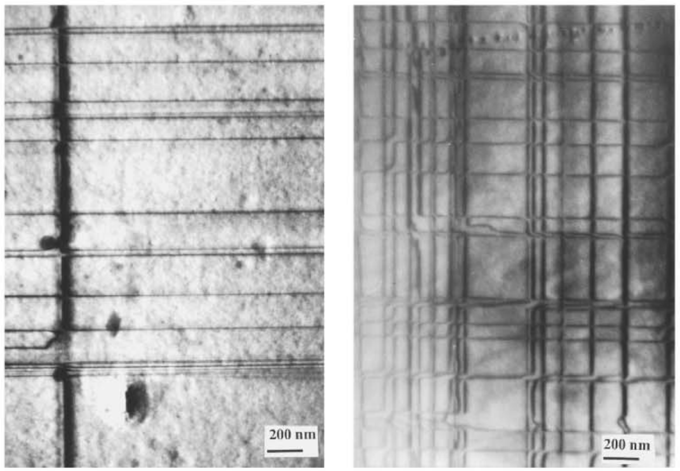

(a) (b)

(001) plan view bright-field zone axis TEM micrographs of two In$_x$Ga$_{1-x}$As/GaAs layers showing the different MD densities along the two <110>-type directions: (a) sample 2, x=0.105, t=68 nm; (b) sample 3, x=0.080, t=200 nm. It is worth noting that the dislocations tend to align in bands even at low density.

Single layer InxGa$_{1-x}$As/GaAs strained structure (110) and (1-10) planar channeling

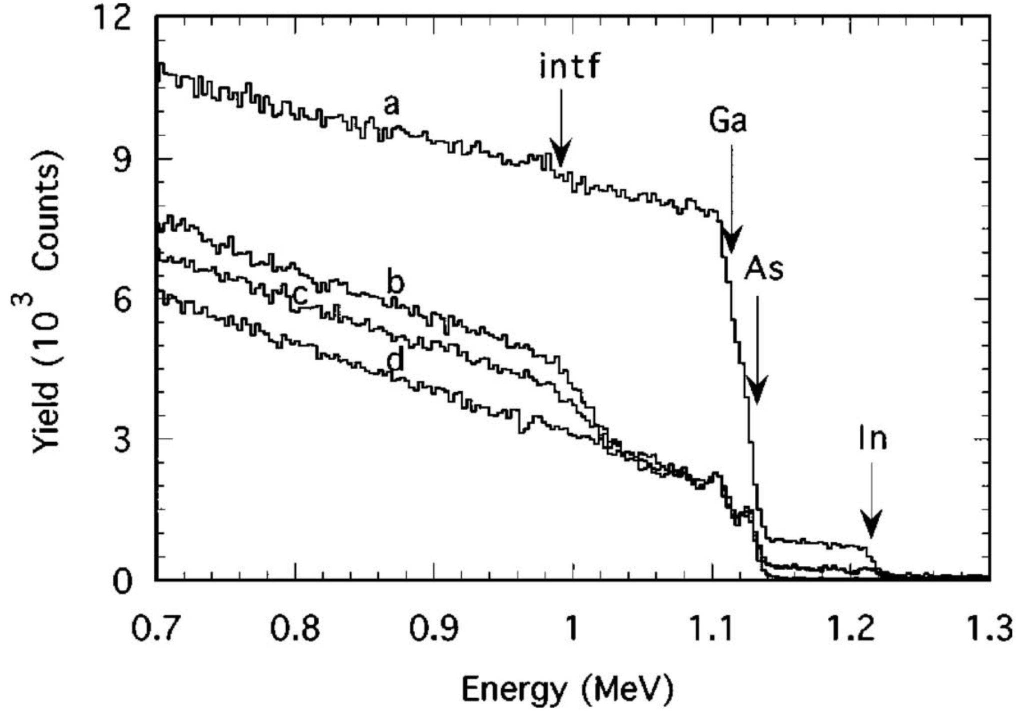

1.4-MeV He RBS spectra of sample 3 and of a GaAs substrate as a reference. The arrows indicate the surface scattering energies from different elements and the position of the interface (intf). Spectra *a*, *b*, and *c* refer to sample 3 and correspond in that order to random, (110), and (1-10) incidence; spectrum *d* GaAs (110) planar channeling.

Mazzer, Drigo, Romanato, Salviati and Lazzarini PRB 56, 6895,1997

Lattice deformation studies

Pseudomorphic epitaxial structures

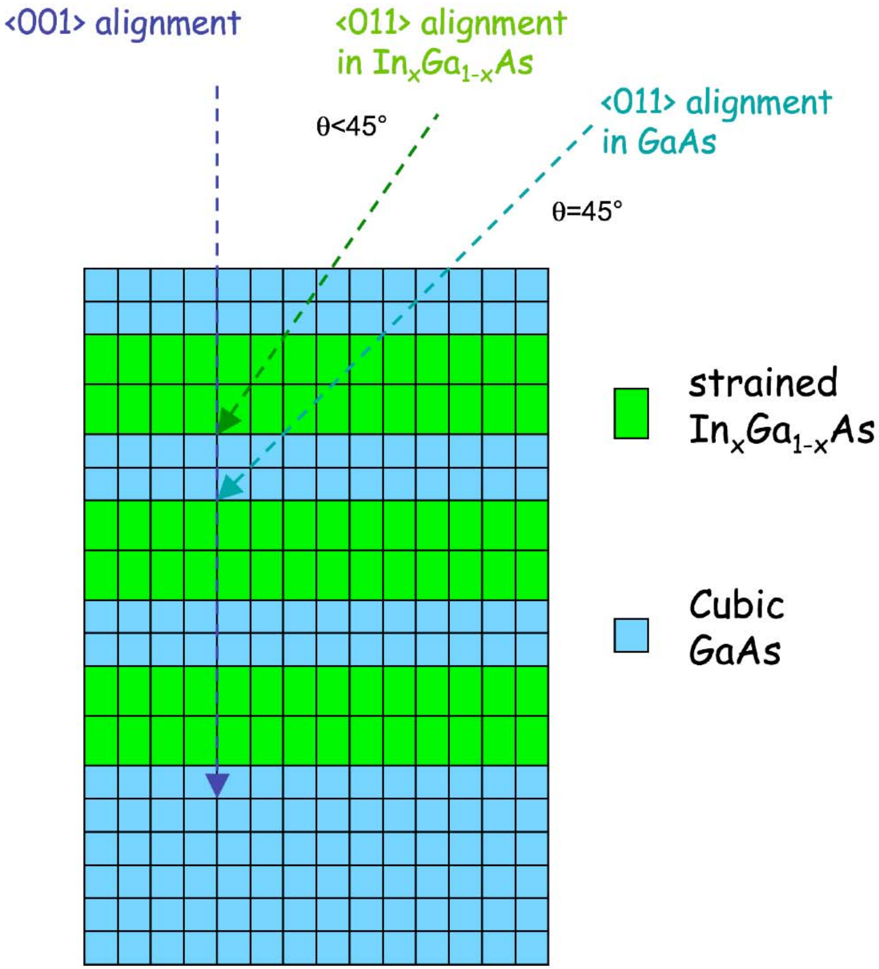

Pseudomorphic epitaxial structures

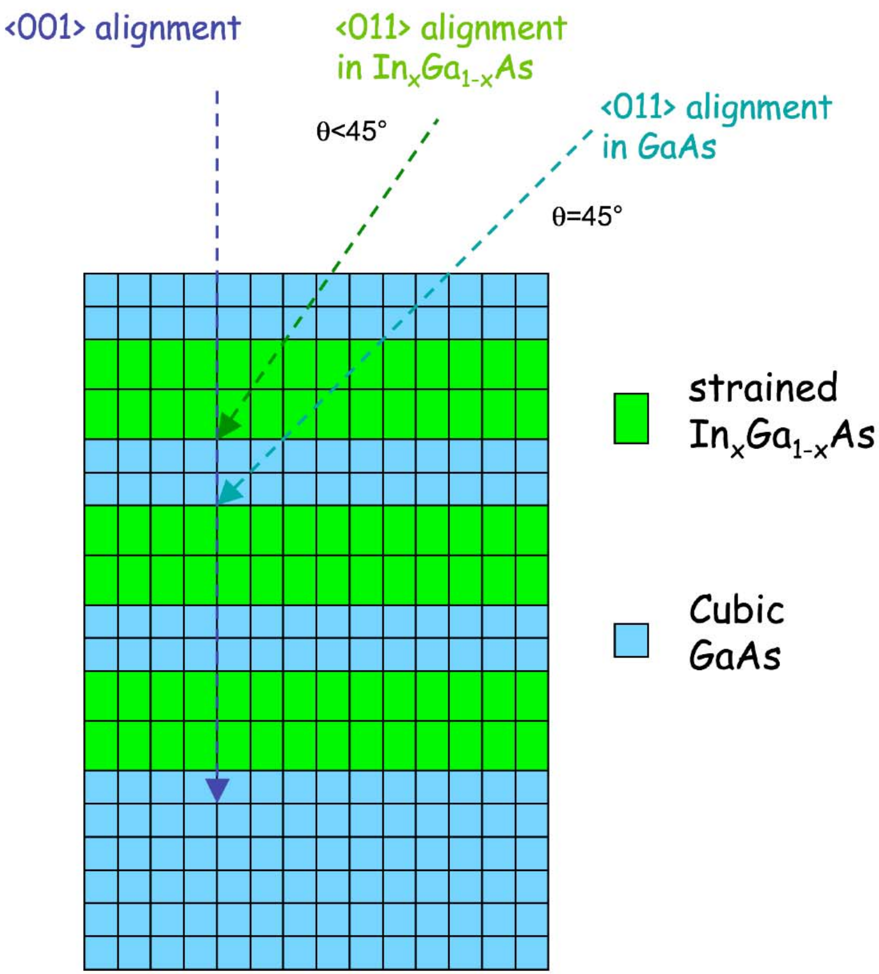

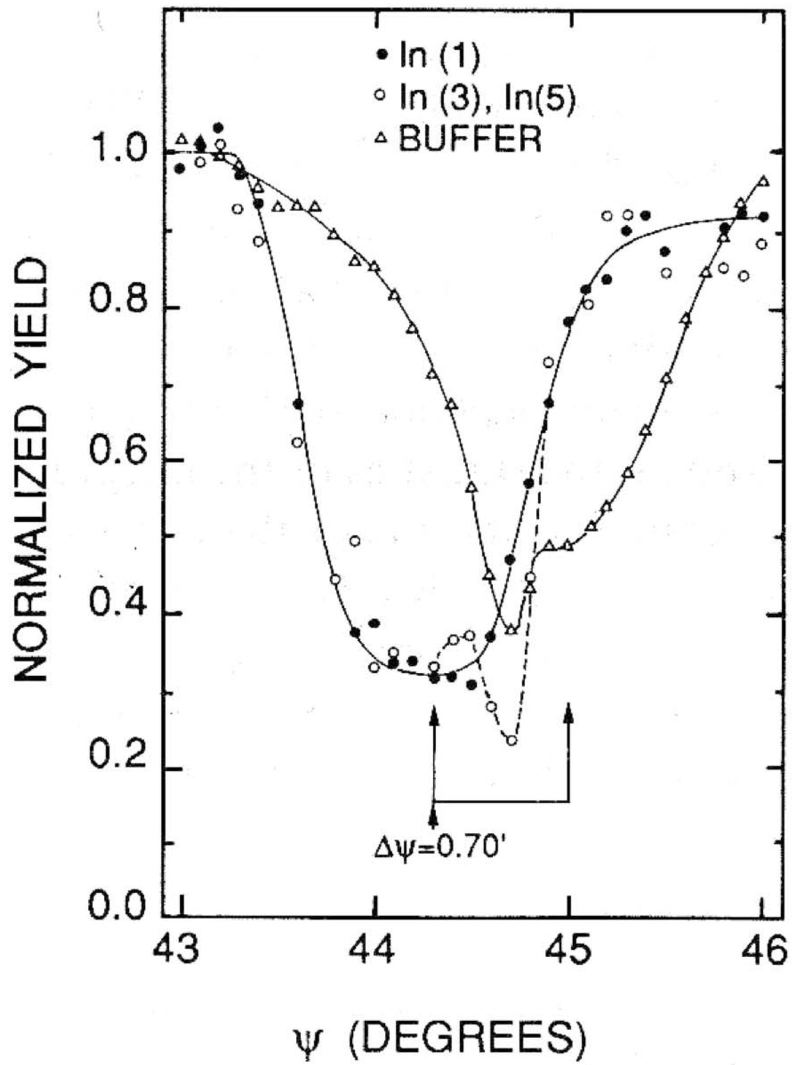

Measurement of lattice strain

A. Camera, A.V. Drigo / Channeling analysis of epitaxial layers

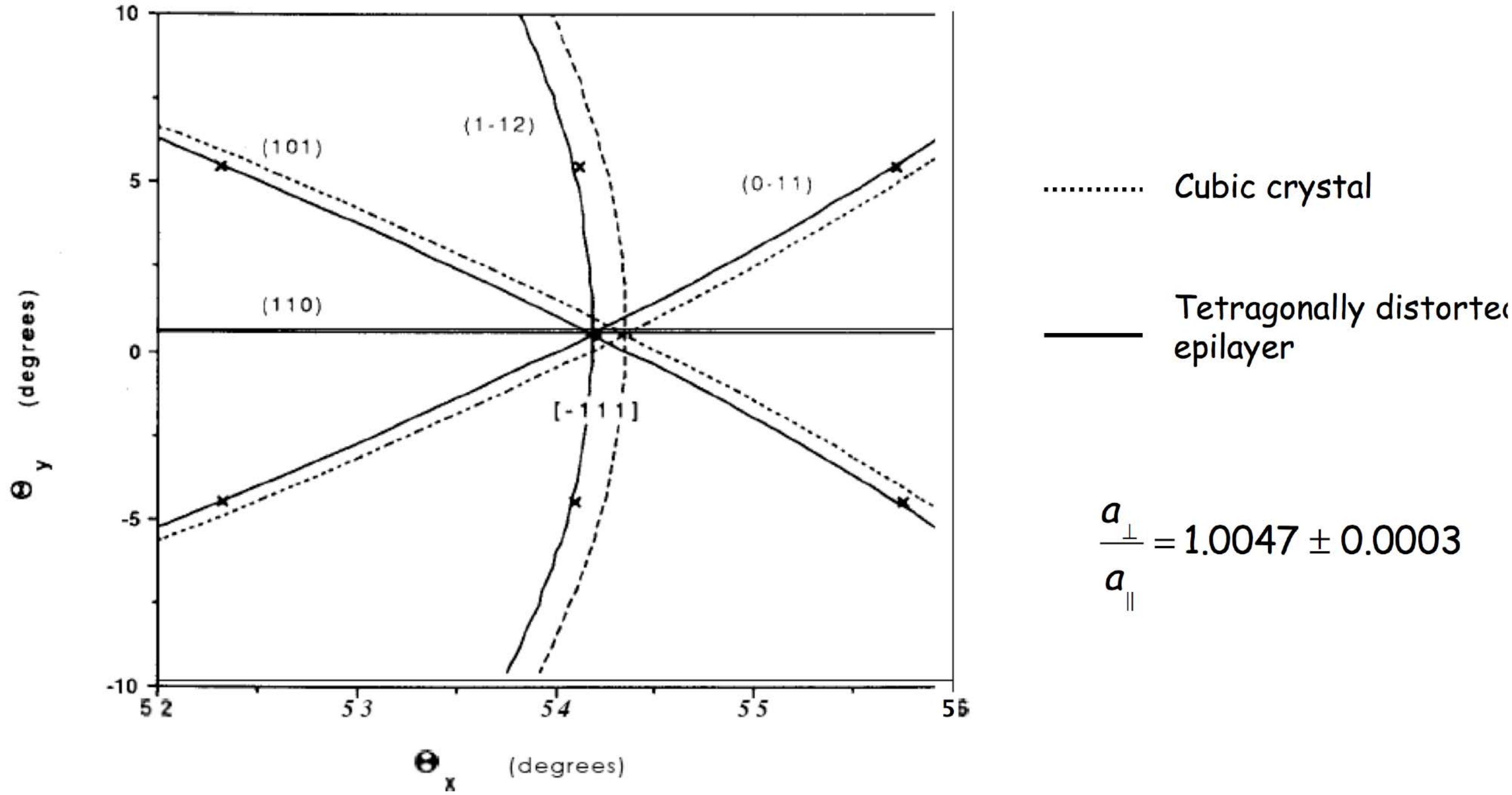

$$\frac{a_\perp}{a_\parallel} = 1.0047 \pm 0.0003$$

Catastrophic dechanneling in strained layers

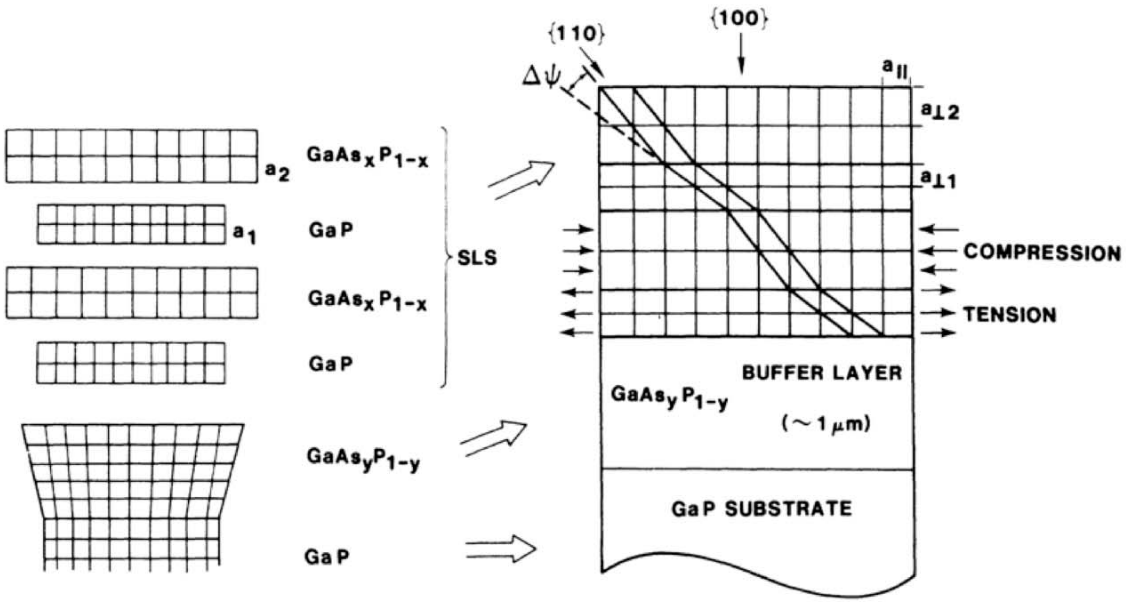

Picraux, Biefeld, Allen, Chu, Ellison PRB 38, 11086, 1988

Catastrophic dechanneling in strained layers

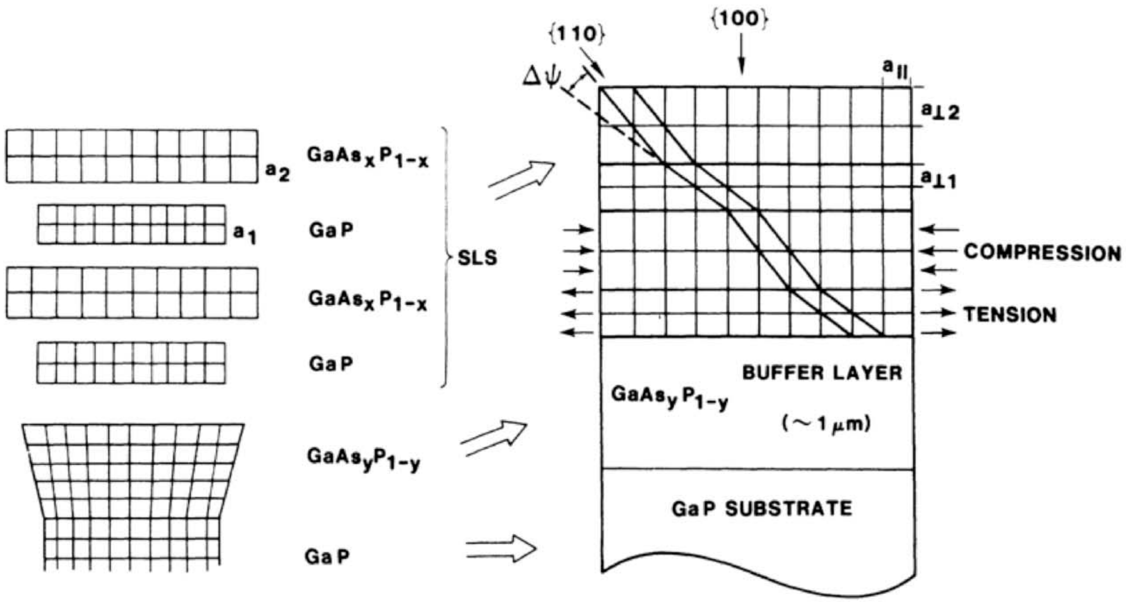

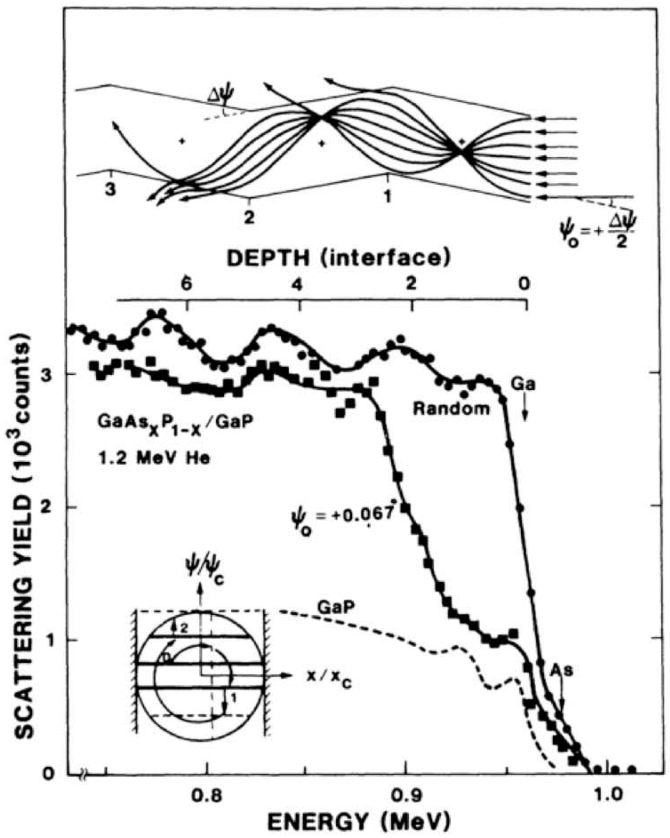

Picraux, Biefeld, Allen, Chu, Ellison PRB 38, 11086, 1988

Influence of the lattice on the ion flux

Channeling flux in TiO_x

<0001> axial channeling

• Ti(d,d)Ti   ○ $^{16}O(d,p)^{17}O$

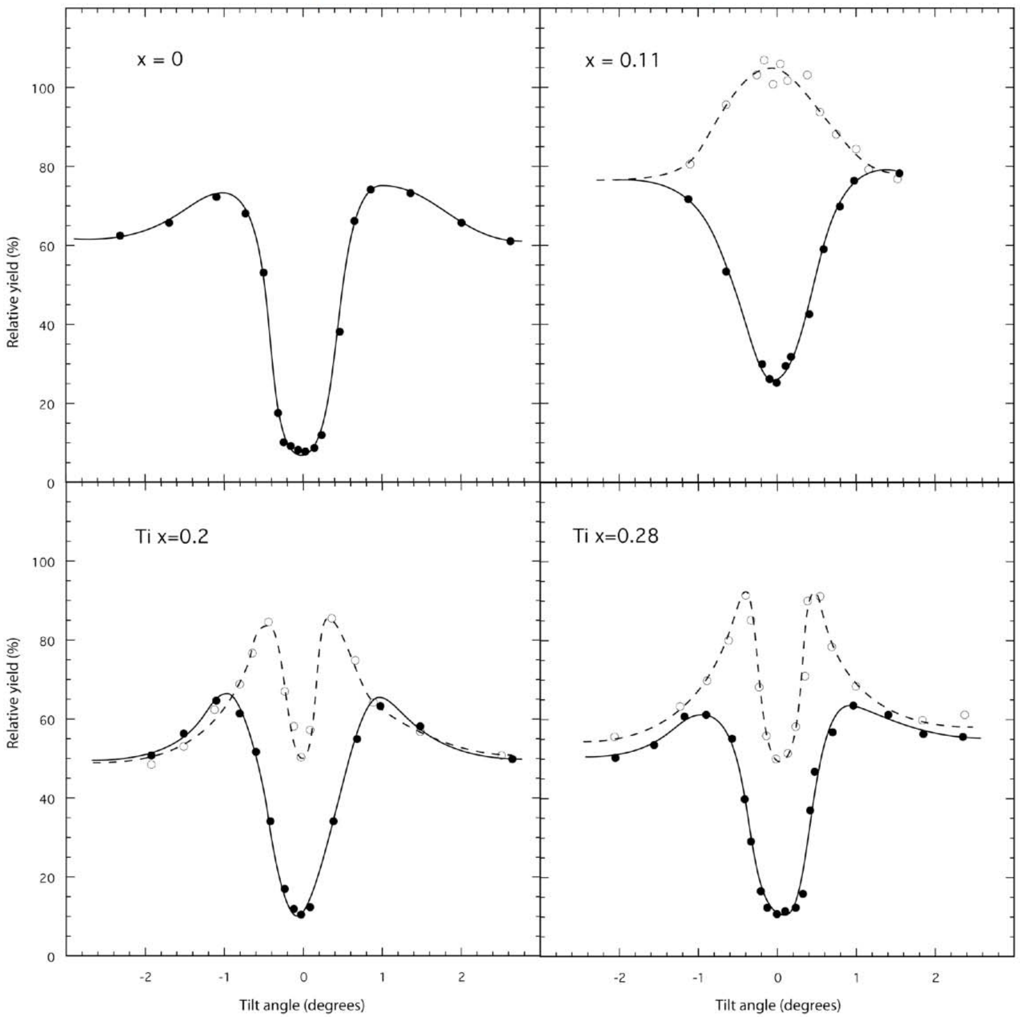

Della Mea, Drigo, Lo Russo, Mazzoldi, Yamaguchi, Bentini, De Salvo and Rosa Phys.Rev. B 10, 1836, 1974

Channeling flux in TiO_x

<0001> axial channeling

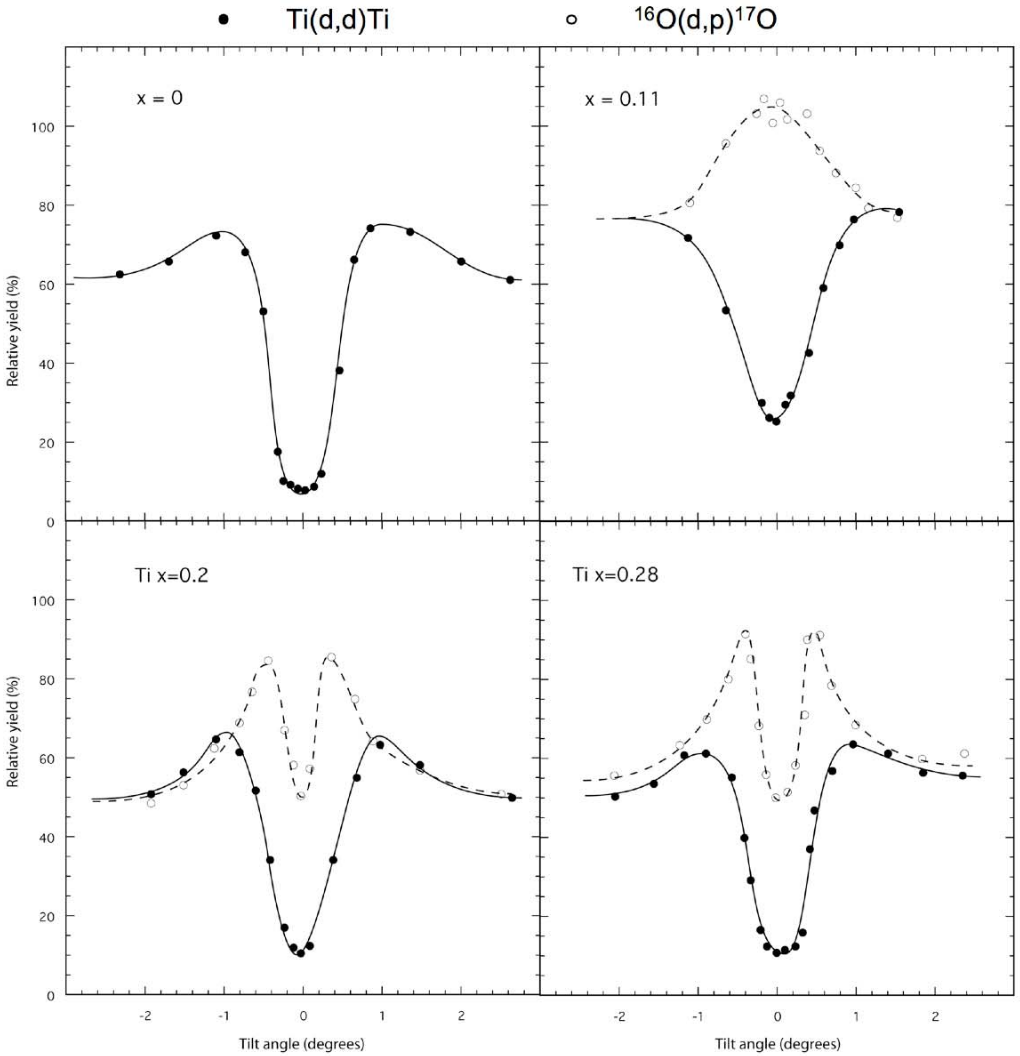

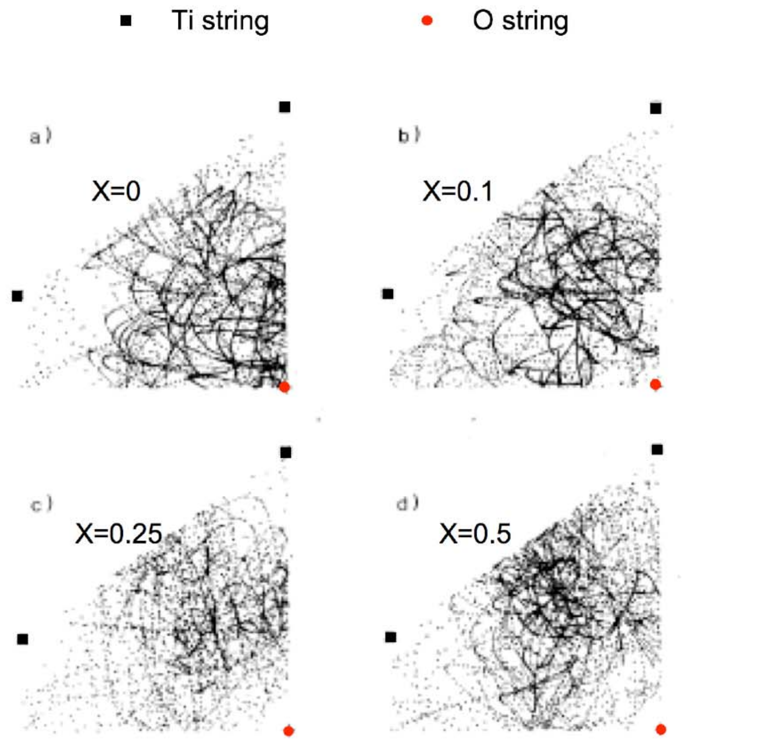

Plot of the Montecarlo trajectories of 1 MeV deuteron impinging parallel to the [110] axis of a TiO_x crystals having different oxygen content.

Della Mea, Drigo, Lo Russo, Mazzoldi, Yamaguchi, Bentini, De Salvo and Rosa Phys.Rev. B 10, 1836, 1974

Feeding-in (volume capture) and blocking of 1 MeV protons in Si thin crystals

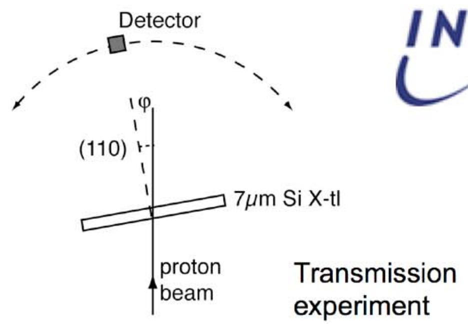

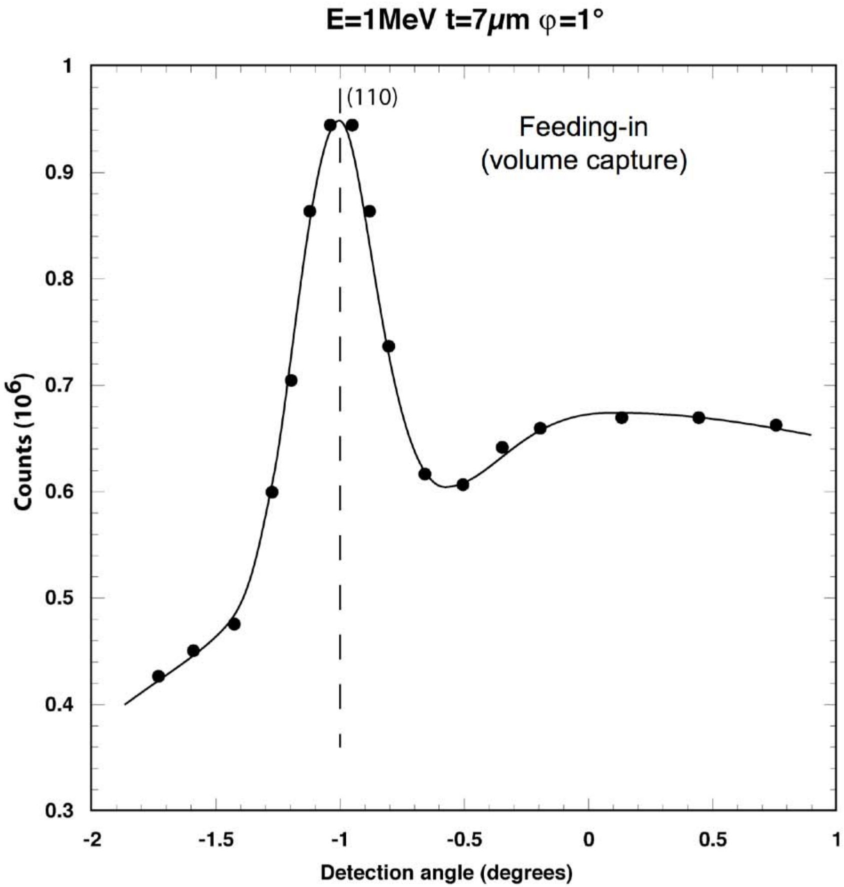

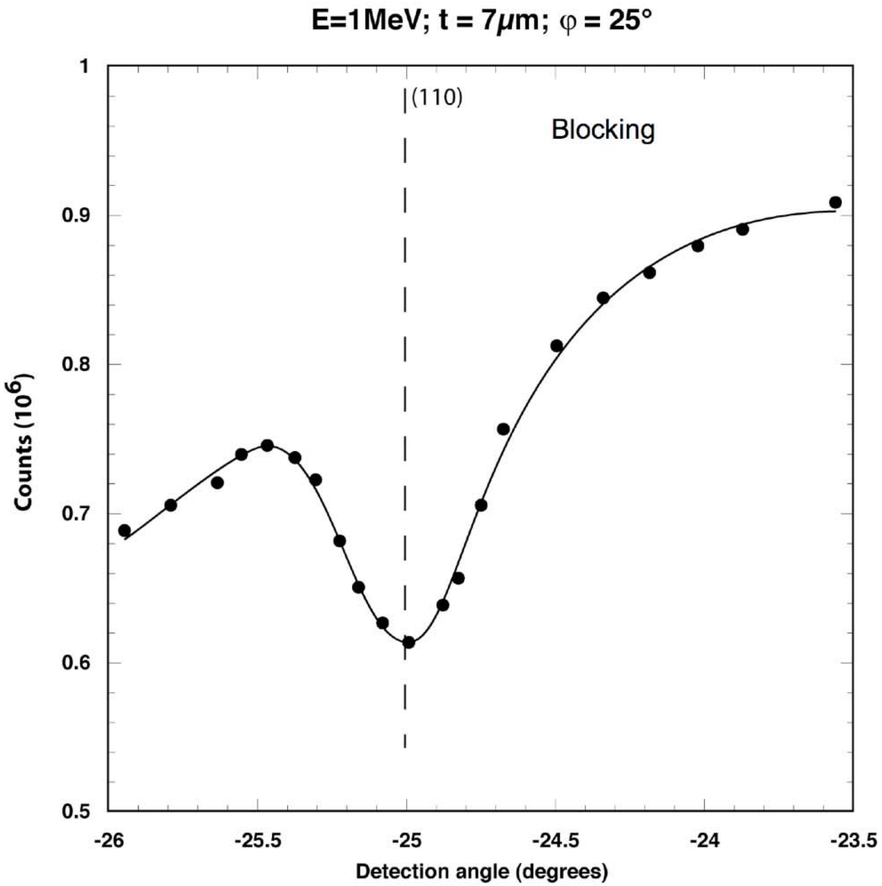

Characterization of crystals for relativistic channeling experiments

Optimization of Si crystals processing

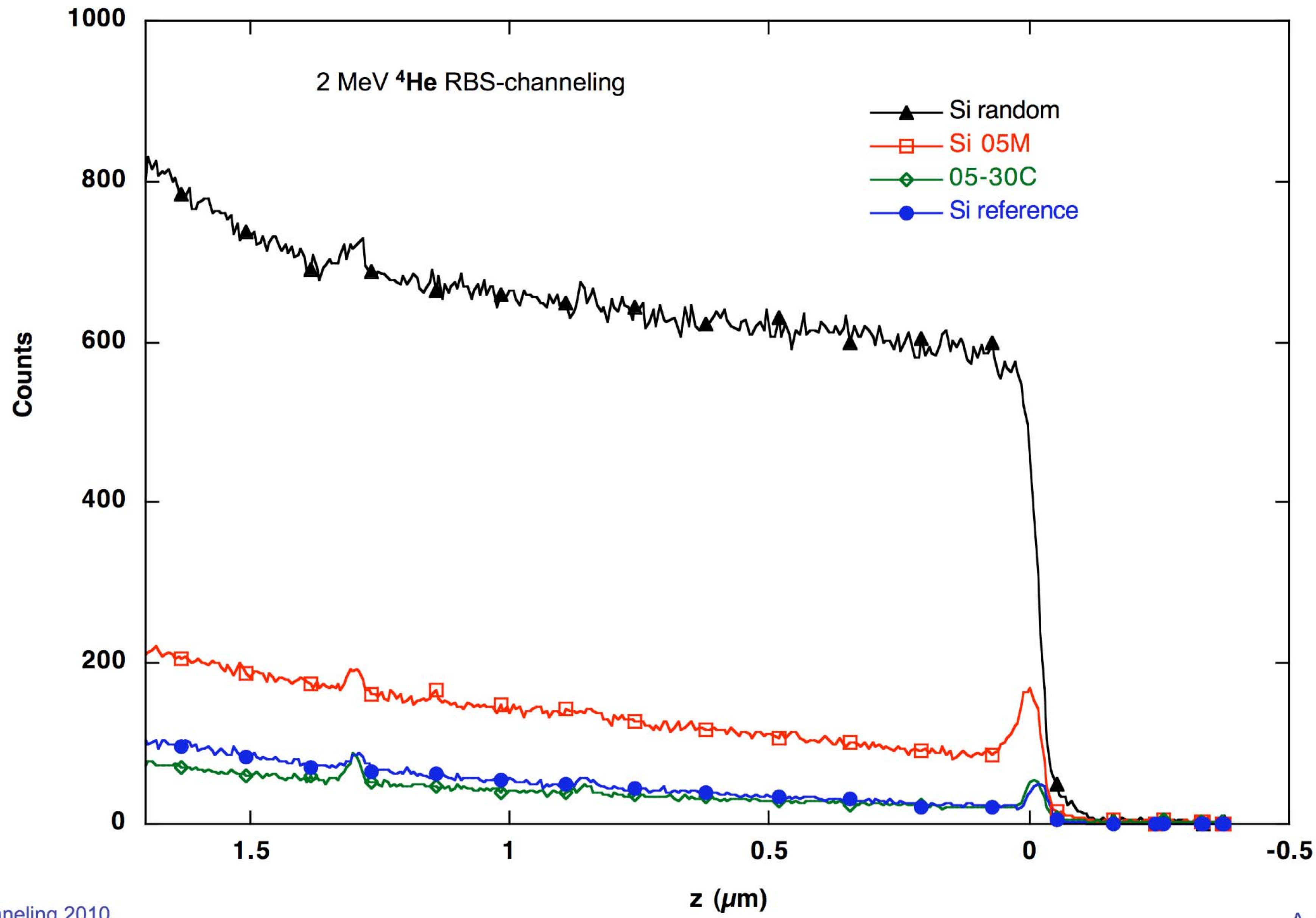

Optimization of Si crystals processing

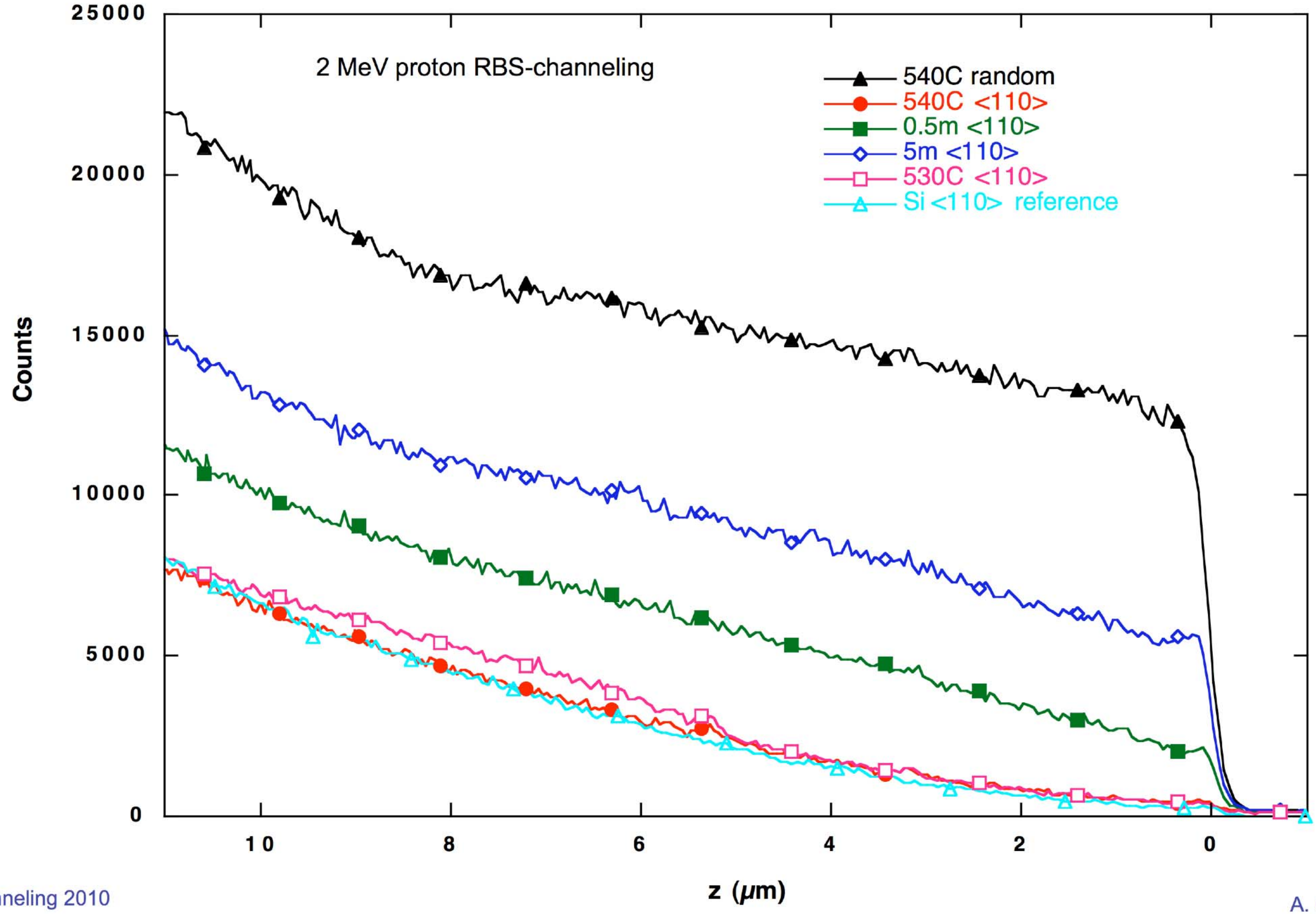

A novel material: $LiNbO_3$

Piezoelectrically tunable beam deflector

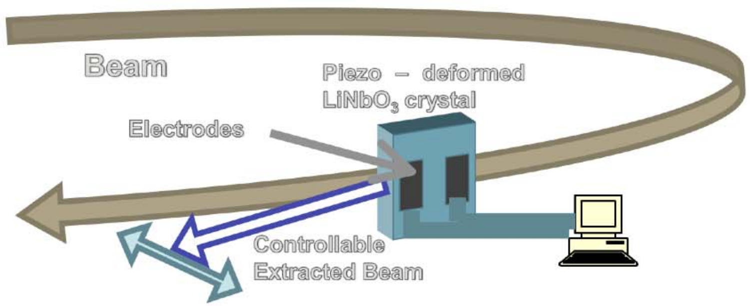

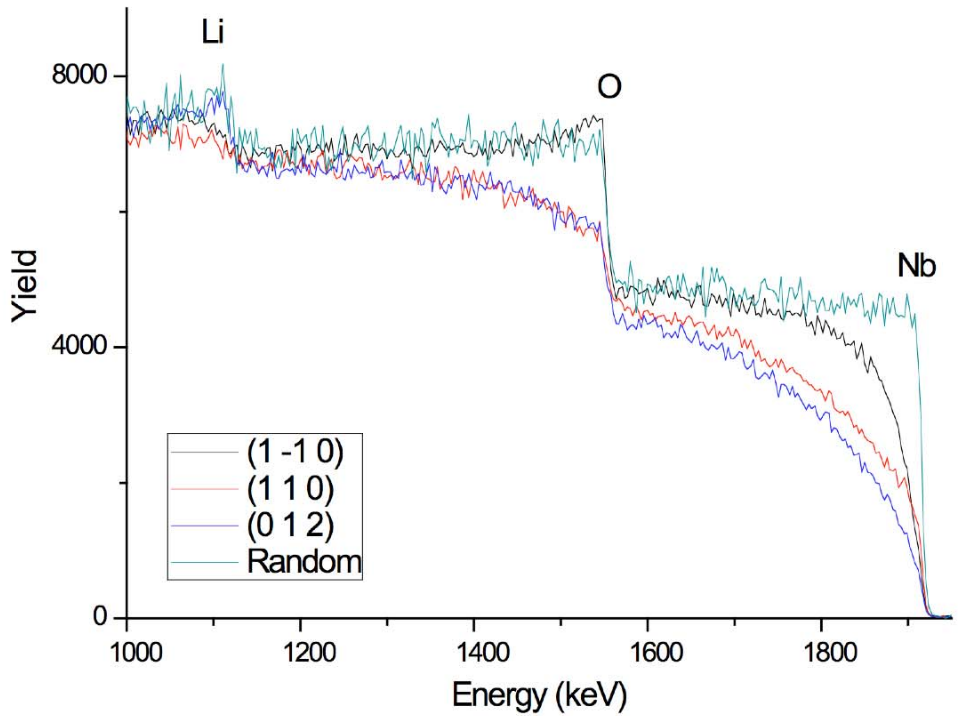

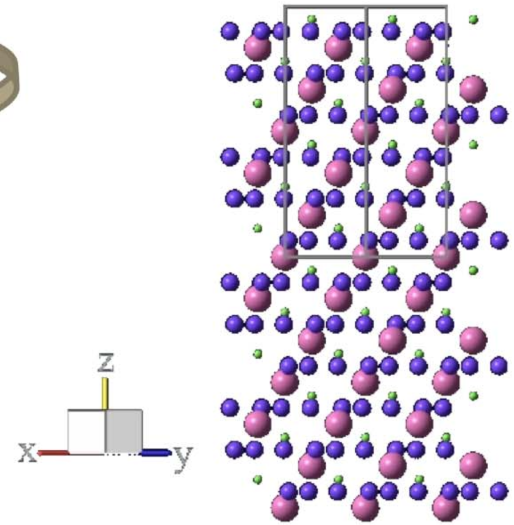

(012) planes

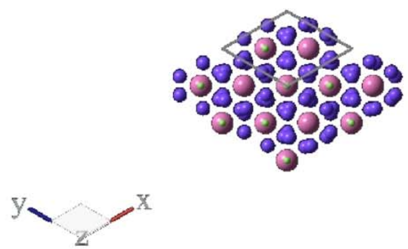

(110) planes

Fe atom location in $LiNbO_3$

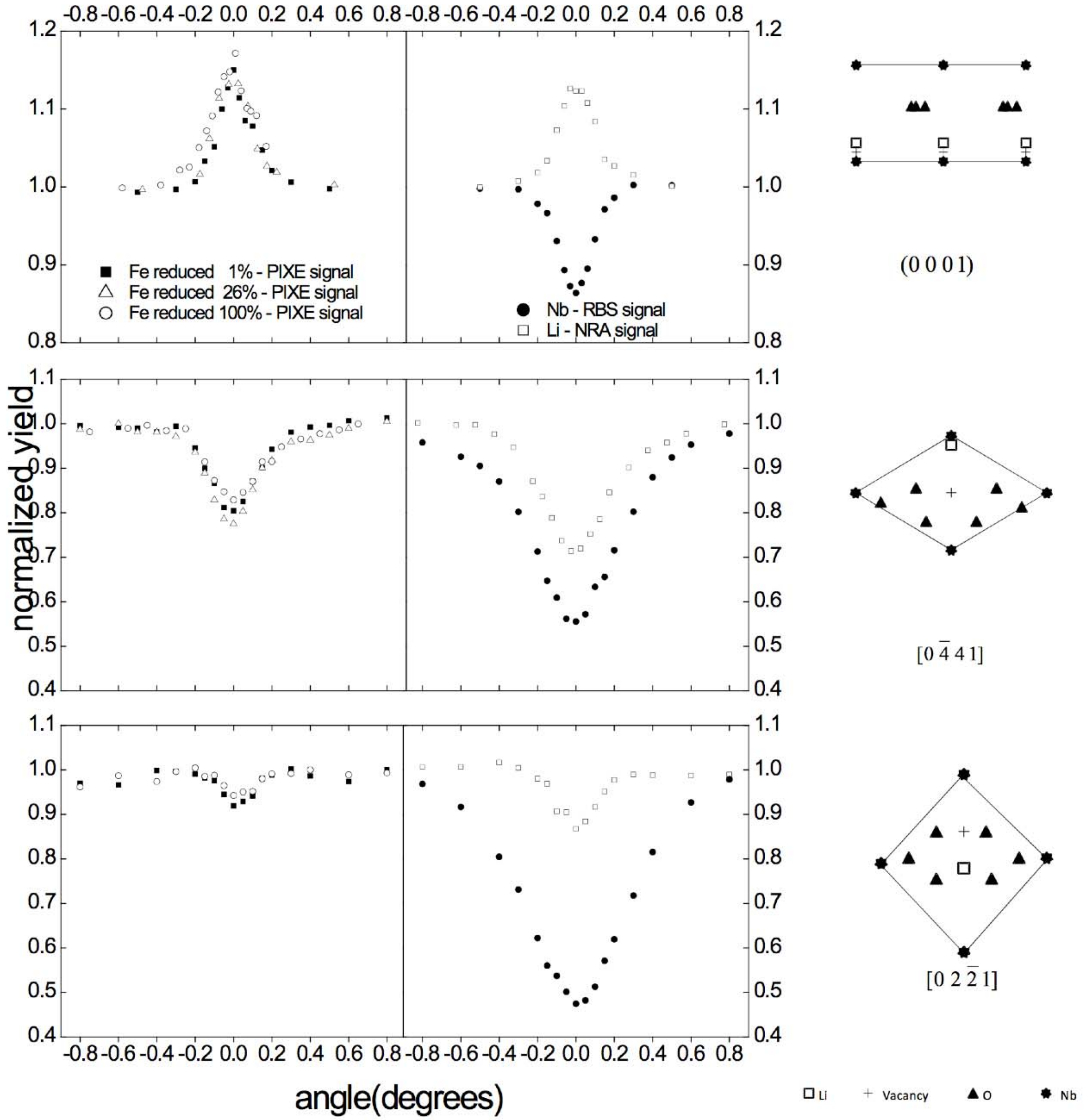

A. Carnera

Conclusions

Conclusions

- MeV energy ions channeling is a well assessed methodology for investigating lattice structures

Conclusions

- MeV energy ions channeling is a well assessed methodology for investigating lattice structures
- It has been, and still it is, one of the most useful tools in the microelectronic and optoelectronic materials R&D

Conclusions

- MeV energy ions channeling is a well assessed methodology for investigating lattice structures
- It has been, and still it is, one of the most useful tools in the microelectronic and optoelectronic materials R&D
- It can provide complementary information with other more traditional crystallographic tools (i.e. X-ray diffraction)

Conclusions

- MeV energy ions channeling is a well assessed methodology for investigating lattice structures
- It has been, and still it is, one of the most useful tools in the microelectronic and optoelectronic materials R&D
- It can provide complementary information with other more traditional crystallographic tools (i.e. X-ray diffraction)
- It can be a key tool for the development of crystal for new exotic applications

Thank you

and

“Long live channeling”